ISSN 2228-9860 eISSN 1906-9642 CODEN: ITJEA8

International Transaction Journal of Engineering, Management, & Applied Sciences & Technologies

http://TuEngr.com

C-UPFC Modeling in NEPLAN for Power Flow Analysis

Ayman Awad [1], Salah Kamel [1], Ali S. Alghamdi [2*], Francisco Jurado [3], Mohamed Zohdy [4]

[1] *Department of Electrical Engineering, Aswan University, Aswan 81542, EGYPT.*

[2] *Department of Electrical Engineering, Faculty of College of Engineering, Majmaah University, Majmaah 11952, SAUDI ARABIA.*

[3] *Department of Electrical Engineering, University of Jaén, 23700 EPS Linares Jaén, SPAIN.*

[4] *Electrical and Computer Engineering Department, School of Engineering and Computer Science, Oakland University, Rochester, MI 48309, USA.*

**Corresponding Author (Tel: +966(16)404-2568 Email: AAlghamdi@mu.edu.sa).*

Paper ID: 12A1F

Volume 12 Issue 1

Received 24 July 2020
Received in revised form 14 October 2020
Accepted 26 October 2020
Available online 03 November 2020

Keywords:
Flexible AC Transmission Systems (FACTS); Center node Unified Power Flow Controller (C-UPFC); NEPLAN software; C-UPFC modeling; Power flow.

Abstract

Center node Unified Power Flow Controller (C-UPFC) is considered as the most recent FACTS device. When attached to the desired transmission line, typically at the midpoint, it influences the flow of active and reactive power through the transmission line, even from its sending and receiving terminals, besides controlling the voltage level of the midpoint that the device is connected. This paper introduces a model for C-UPFC in NEPLAN software, aimed to be utilized for power flow analyses incorporating this device in power systems. It is designed using the components available on the utilized software so that it can be integrated with case studies tests and analyses performed by such software. The power injection method is used in designing the model to facilitate the calculations for analyses involving the device. A test is carried out to this model on IEEE 30 bus and IEEE 14 bus power systems to guarantee its quality in different cases for each system.

Disciplinary: Electrical Engineering and Technology.

Cite This Article:

Awad, A., Kamel S., Alghamdi, A.S., Jurado, F., Zohdy, M. (2021). C-UPFC Modeling in NEPLAN for Power Flow Analysis. *International Transaction Journal of Engineering, Management, & Applied Sciences & Technologies, 12*(1), 12A1F, 1-11. http://TUENGR.COM/V12/12A1F.pdf DOI: 10.14456/ITJEMAST.2021.6

Nomenclature

C-UPFC	Center-node Unified Power Flow Controller
FACTS	Flexible AC Transmission systems
IPFC	Interline Power Flow Controller

p.u.	Per Unit
P	Active power
Q	Reactive power
S	Apparent power
SSSC	Static Synchronous Series Compensator
STATCOM	Static Synchronous Compensator
TL	Transmission Line
UPFC	Unified Power Flow Controller
VSC	Voltage Source Converter
V_R	Receiving voltage source
V_S	Sending voltage source
V_{Sh}	Shunt voltage source
X_R	Impedance of Receiving voltage source
X_S	Impedance of Sending voltage source
X_{Sh}	Impedance of Shunt voltage source

1 Introduction

Flexible AC Transmission Systems (FACTS) is a well-known technology that is utilized in the few last decades to control a transmission line and improve its stability, transferability, and performance improvement of a power system in general. With the advance of power electronics through the last years, DC-links with VSCs enabled the utilization of DC storage in FACTS devices, replacing passive components used before, like capacitors and reactors [1]. Hence, FACTS technology achieved development, resulting in a variety of advanced FACTS devices with superior capabilities, including STATCOM, SSSC, IPFC, and UPFC varieties [1-5]. One of the most recent and spectacular FACTS device developed is C-UPFC. It is said to be one of the most powerful FACTS devices. It is mounted to the middle, typically the transmission line midpoint, and hence, it has the capability of controlling the flow of active and reactive energy from end-to-end of the line, and the voltage level of the midpoint as well [11, 12].

The modeling of such devices in different simulation software is attracting the intention of many. In [6] and [7], the STATCOM model is presented using MATLAB software involving the Newton-Raphson load flow algorithm. While in [8] and [9], the SSSC model is presented, wherein [9], SSSC modeling was presented in MATLAB software, while in [9] it is implemented using NEPLAN software. The work [10] presents a model of IPFC using MATLAB regarding the Newton-Raphson algorithm for load flow.

For involving C-UPFC regarding power system analysis, few contributions were presented. In [11], a C-UPFC model is proposed with a control design for performance enhancement of C-UPFC regarding power transmission applications. In [12], another C-UPFC model is proposed using only one voltage source converter instead of three voltage source converters, where this model is implemented by PSCAD software for transient analyses. In [13], a C-UPFC model is proposed for performance improvement of induction-based wind farms, where this model is implemented using

MATLAB Simulink software. In [14] and [15], modeling of C-UPFC is introduced by MATLAB software involving the Newton-Raphson algorithm for load flow.

This paper introduces a C-UPFC model for power flow analysis, where it is implemented by NEPLAN software. Injection of active and reactive power to a system is the dependable technique for such a model, and it is established by NEPLAN software existed components. This model can help to calculate the desired analyses incorporating C-UPFC in power systems. It was assessed on IEEE 14 bus and IEEE 30 bus power systems in different test conditions, where the control values and location of installation are varied so that the robustness of such a model is ensured.

2 C-UPFC Structure

Due to the importance of power flow regulation and voltage control, UPFC was innovated. However, it has a drawback, that it can regulate power flow from one side of the transmission line only i.e. even the sending terminal or the receiving terminal. Figure 1 shows the schematic diagram of the UPFC.

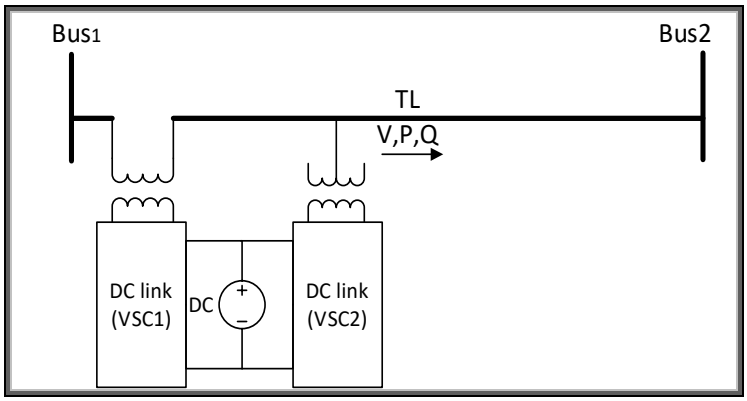

Figure 1: Schematic diagram of UPFC

For overriding such a drawback, C-UPFC was innovated by Olorunfemi Ojo and Sanbao Zheng [6]. It is mainly designed to be installed at the desired TL midpoint. It consists of a DC source, three DC-links, three coupling transformers, where these transformers are two series transformers and a shunt transformer. The series transformers are responsible for controlling the flow of active and reactive power from-end-to-end of the TL, while the shunt transformer – connected to the center node of the TL – responsible for voltage regulation. The schematic diagram shown in Figure 2 shows the structure and connection of C-UPFC.

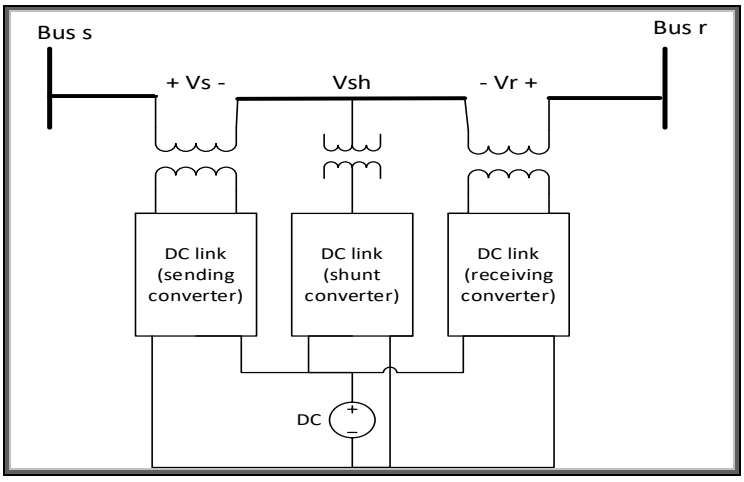

Figure 2: Schematic diagram of C-UPFC

This connection offers exceptional capabilities for C-UPFC. Power transfer maximization can be gained while controlling active and reactive power flow in both sending and receiving ends, besides voltage regulation of the line through the center node. Such a device can be modeled as follows: each DC-link and coupling transformer can be represented as an injected voltage source and an impedance, where two of them are series-connected to the transmission line, while all of them are shunt-connected to the center node, where 3 auxiliary buses are inserted, as shown in Figure 3.

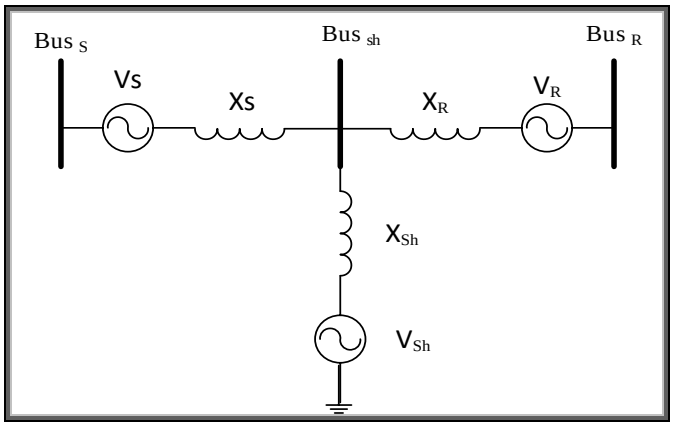

Figure 3: Equivalent circuit of C-UPFC.

Through the injected voltage by sources V_S and V_R, the power flow control is carried out, while the voltage of the center node is controlled by the injected current of V_{Sh}.

3 C-UPFC modeling

Due to Figures 2 and 3, the representation of C-UPFC in a TL would result in "dividing" the transmission line into two equal sections, where C-UPFC is inserted between these two sections. The model contains three auxiliary buses: two for the sending and receiving series DC links, and one for the shunt DC link, as shown in Figure 4.

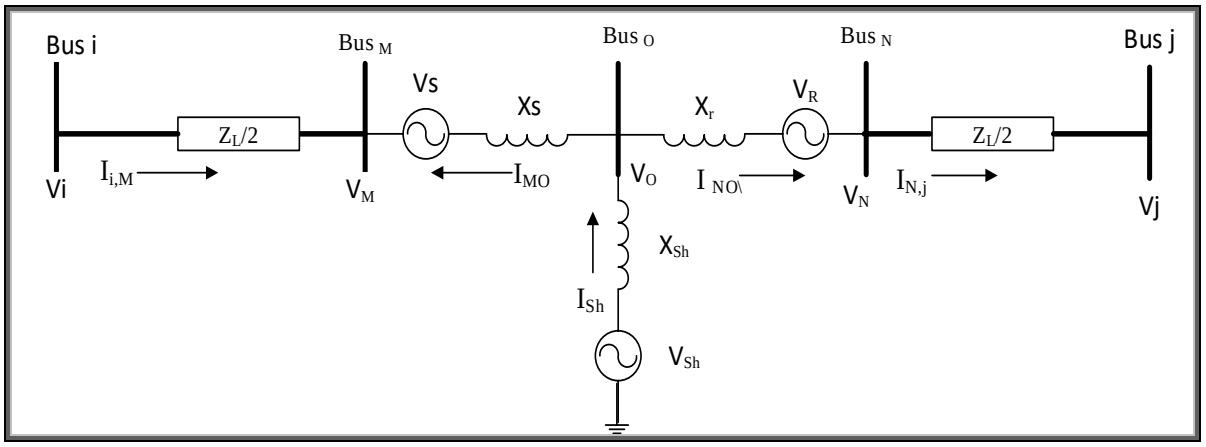

Figure 4: Modeling of C-UPFC

Applying Kirchhoff's current law on sending bus (Bus_s):

$$I_S = I_{MO} - I_{i,M} = \left(\frac{V_M - V_O}{jX_S}\right) - \left(\frac{S_{i,M}}{V_M}\right)^* \quad (1)$$

where I_S is total current sent from bus i to bus M, I_{MO} is the current injected to the line i_M by the sending DC link, $I_{i,M}$ is the current of line i_M, $S_{i,M}$ is power flow through line i_M, and

$$S_{i,M} = P_{i,M} + Q_{i,M} \quad (2).$$

Applying Kirchhoff's current law on sending bus (Bus_r)

$$I_R = I_{NO} - I_{N,j} = \left(\frac{S_{N,j}}{V_N}\right)^* + \left(\frac{V_N - V_O}{jX_r}\right) \quad (3),$$

where I_R is total current sent from bus N to bus j, I_{NO} is the current injected to the line N_j by the receiving DC link, $I_{N,j}$ is the current of line Nj, $S_{N,j}$ is power flow through line N,j, and:

$$S_{N,j} = P_{N,j} + Q_{N,j} \quad (4).$$

Applying Kirchhoff's current law on the center node (Bus_O), then

$$I_{Sh} = I_{MO} + I_{NO} \quad (5)$$

and

$$V_{Sh} = I_{Sh} * jX_{Sh} \quad (6).$$

Due to the illustrated equations above, the model can fulfill the duties of the C-UPFC device i.e. flow controlling of active and reactive power over the line, and voltage level controlling of the center node.

4 Model simulation and testing

This model is put on tests in both IEEE 14 bus and IEEE 30 bus standard power systems, two cases each, where the model is installed in a different position for each case with different control settings.

4.1 Testing in IEEE 14 Bus Power System

This system consists of 14 buses, 20 transmission lines, 5 generators, and 11 loads [16]. C-UPFC model is tested in that system in two cases as follows:

- Case (1): Controlling line 4 (connecting buses 2 and 4) with settings of active power P= 50 MW, reactive power Q= 25 MVAr, and center node voltage V_{Sh}=1.0145 p.u.
- Case (2): Controlling line 5 (connecting buses 2 and 5) with settings of active power P= 40 MW, reactive power Q= 25 MVAr, and center node voltage V_{Sh}=1.0435 p.u.

Figure 5 shows the integration of C-UPFC in NEPLAN software on the system, and Table 1 presents the results of voltage control, while Table 2 presents the results of power flow control on each TL in each case.

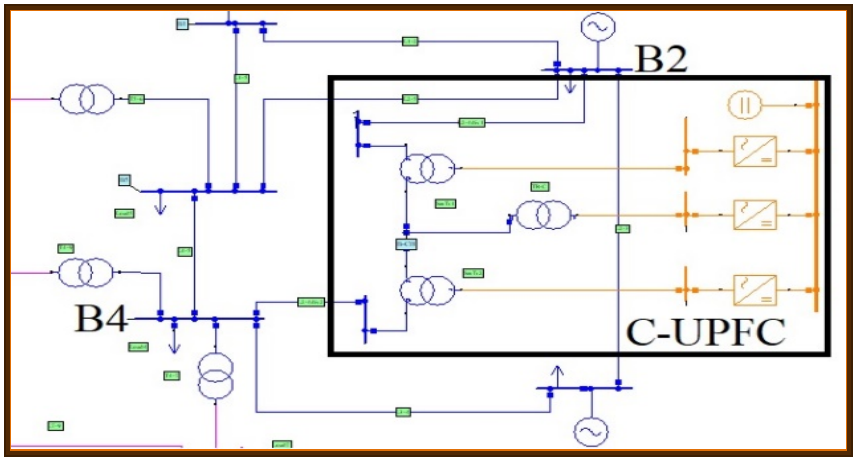

Figure 5: Implemented C-UPFC model integration on IEEE 14 bus power system

Table 1: Results of voltage control of the IEEE 14 bus power system

Bus no.	Base case V(p.u.)∠ɵ°	Case (1) V(p.u.)∠ɵ°	Case (2) V(p.u.)∠ɵ°
1	1.06 ∠0.0°	1.06 ∠0.0°	1.06 ∠0.0°
2	1.045 ∠-5°	1.045 ∠-4.8°	1.045 ∠-4.9°
3	1.01 ∠-12.8°	1.01 ∠-12.8°	1.01 ∠-12.7°
4	1.012 ∠-10.2°	1.0223 ∠-10.7°	1.0172 ∠-10.3°
5	1.016 ∠-8.7°	1.0213 ∠-9.0°	1.0259 ∠-8.9°
6	1.07 ∠-14.4°	1.07 ∠-14.7°	1.07 ∠-14.5°
7	1.048 ∠-13.2°	1.0539 ∠-13.6°	1.0517 ∠-13.3°
8	1.09∠-13.2°	1.09∠-13.6°	1.09∠-13.3°
9	1.032 ∠-14.8°	1.037 ∠-15.2°	1.035 ∠-14.9°
10	1.031 ∠-15°	1.0353 ∠-15.4°	1.0337 ∠-15.1°
11	1.047 ∠-14.8°	1.0489 ∠-15.1°	1.0481 ∠-14.9°
12	1.053 ∠-15.3°	1.0538 ∠-15.5°	1.0536 ∠-15.3°
13	1.047 ∠-15.3°	1.0476 ∠-15.6°	1.0473 ∠-15.4°
14	1.02 ∠-16.1°	1.0234∠-16.4°	1.0222∠-16.1°
V_{CP}	-	1.0145 ∠9.5°	1.0435 ∠7.6°
V_S	-	1.0035 ∠-6.8°	1.0066 ∠-6.4°
V_R	-	1.0572 ∠-8.7°	1.0577 ∠-7.5°

Table 2: Results of power flow control of IEEE 14 bus power system on each branch

TL x-y	Base case		Case (1)		Case (2)	
	P (MW)	Q (MVAr)	P (MW)	Q (MVAr)	P (MW)	Q (MVAr)
1-2	157.1	-20.5	154.4	-9.26	155.6	-9.52
1-5	75.5	5.6	77.5	2.87	76.49	0.797
2-3	73.5	3.5	74.53	0.324	73.17	0.441
2-4	55.9	1.8	-	-	56.58	-4.63
$2\text{-}4_{S\text{-}R}$	-	-	**50**	**25**	-	-
2-5	41.7	3.4	44.01	-4.041	-	-
$2\text{-}5_{S\text{-}R}$	-	-	-	-	**40**	**25**
3-4	-23.1	6.9	-22.08	0.072	-23.36	3.703
4-5	-59.6	9.1	-63.66	22.94	-59.7	-2.23
4-7	27.2	-5.9	-22.08	0.072	27.41	-5.08
4-9	15.5	2.9	-63.66	22.94	15.63	3.392
5-6	45.8	10.9	-22.08	0.072	45.33	15.65
6-11	8.2	8.7	-63.66	22.94	7.98	8.01
6-12	8.1	3.2	-22.08	0.072	8.0	3.07
6-13	18.3	9.9	-63.66	22.94	18.16	9.52
7-8	0	-23.1	-22.08	0.072	0	-22.9
7-9	27.2	15.7	27.13	16.54	27.41	16.29
9-10	4.5	-0.7	4.407	0.47	4.68	-0.07
9-14	8.7	0.47	8.713	1.205	8.86	0.854
10-11	-4.6	-6.5	-4.6	-5.35	-4.33	-5.89
12-13	-1.9	-1.37	-1.84	-1.22	1.819	-1.303
13-14	-6.3	-4.73	6.37	4.17	6.224	4.534

For both cases, the model proves its effectiveness and robustness. In case (1), the load flow analysis was settled after 10 iterations, and, in case (2) the load flow was settled after 11 iterations. Figure 6 shows the load flow iterations graph for each case.

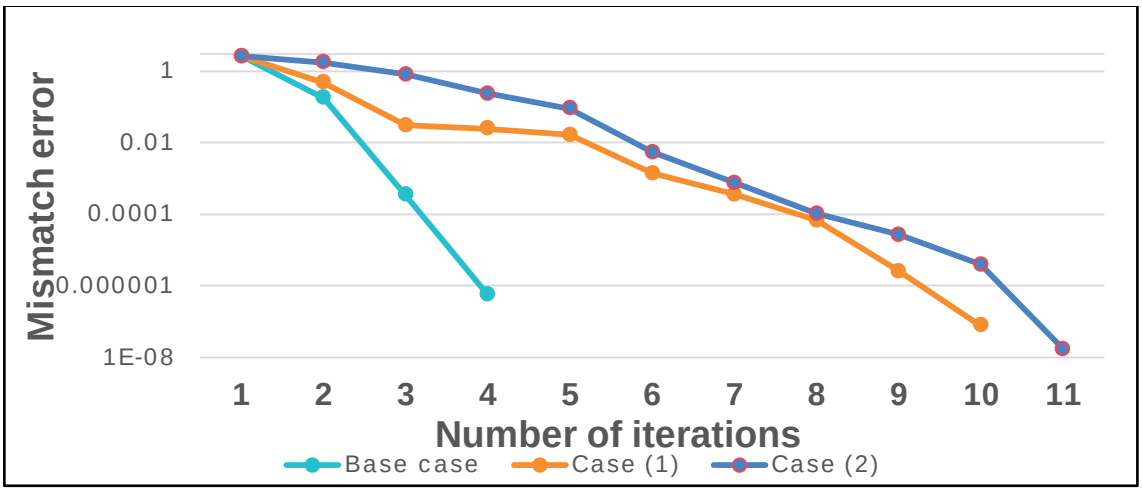

Figure 6: Load flow process iterations for IEEE 14 bus power system cases.

4.2 Testing in IEEE 30 Bus Power System

This system consists of 30 buses, 41 transmission lines, 5 generators, and 22 loads [17]. C-UPFC model is tested in this system in two cases as follows:

- Case (1): Controlling line 6 (connecting buses 2 and 6) with settings of active power P= 90 MW, reactive power Q= 40 MVAr, and center node voltage VSh=1.0227.
- Case (2): Controlling line 9 (connecting buses 6 and 7) with settings of active power P=60 MW, reactive power Q=-10 MVAr, and center node voltage VSh=1.0455.

Figure 7 shows the integration of C-UPFC in NEPLAN software on the system.

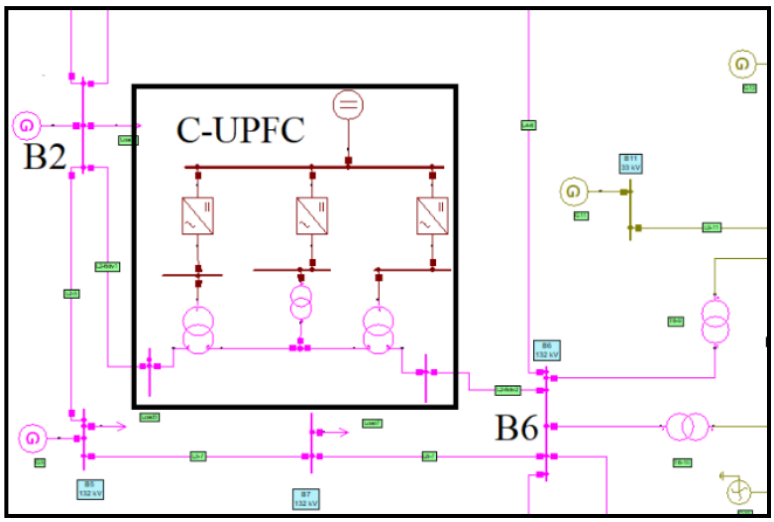

Figure 7: Implemented C-UPFC model integration on IEEE 30 bus power system

Table 3 presents the results of voltage control of the system buses, and Table 4 presents the results of power flow control on each TL in each case.

Again, the good performance of the model is shown in both cases, where the load flow analysis was settled after 7 iterations, for each case. Figure 8 shows the load flow iterations graph for each case.

Table 3: Results of voltage control of the IEEE 30 bus power system

Bus no.	Base case V(p.u.)∠θ°	Case (1) V(p.u.)∠θ°	Case (2) V(p.u.)∠θ°
1	1.06 ∠0.0°	106 ∠0.0°	1.06 ∠0.0°
2	1.043 ∠-5.3°	1.043 ∠-5.4°	1.043 ∠-2.5°
3	1.021 ∠-7.6°	1.028 ∠-7.3°	1.026 ∠-3.7°
4	1.012 ∠-9.3°	1.0168 ∠-9.4°	1.0173 ∠-4.5°
5	1.01∠-14.1°	1.01 ∠-13.8°	1.01 ∠-8.1°
6	1.011 ∠-11°	1.0208 ∠-10.5°	1.0154 ∠-4.8°
7	1.003 ∠-12.8°	1.0087 ∠-12.4°	1.0121 ∠-4.9°
8	1.01∠-11.8°	1.01 ∠-11.1°	1.01 ∠-5.4°
9	1.057 ∠-16°	1.0613 ∠-15.6°	1.0596 ∠-10.1°
10	1.048 ∠-17°	1.0529 ∠-16.6°	1.0512 ∠-11.1°
11	1.082 ∠-16°	1.082 ∠-15.6°	1.082 ∠-10.1°
12	1.059 ∠-15.5°	1.0613 ∠-5.3°	1.0606 ∠-10.2°
13	1.071 ∠-15.5°	1.071 ∠-15.3°	1.071 ∠-10.2°
14	1.045 ∠-16.5°	1.0473 ∠-6.2°	1.0463 ∠-11.0°
15	1.04 ∠-16.6°	1.0431 ∠-6.4°	1.0421 ∠-11.1°
16	1.046 ∠-16.4°	1.0498 ∠-6.1°	1.0488 ∠-10.8°
17	1.043 ∠-17°	1.047 ∠-16.7°	1.0456 ∠-11.3°
18	1.031 ∠-17.5°	1.0344 ∠-17.1°	1.0332 ∠-11.8°
19	1.028 ∠-17.7°	1.0324 ∠-17.4°	1.0311 ∠-12°
20	1.032 ∠-17.6°	1.0367 ∠-17.3°	1.0353 ∠-11.9°
21	1.036 ∠-17.4°	1.0406 ∠-17.0°	1.0389 ∠-11.5°
22	1.036 ∠-17.3°	1.0411 ∠-16.9°	1.0394 ∠-11.5°
23	1.03 ∠-17.1°	1.0339 ∠-16.8°	1.0326 ∠-11.5°
24	1.025 ∠-17.4°	1.0301 ∠-17.0°	1.0282 ∠-11.6°
25	1.022 ∠-16.6°	1.0283 ∠-16.2°	1.0257 ∠-10.6°
26	1.003 ∠-17.1°	1.0108 ∠-16.6°	1.0082 ∠-11.1°
27	1.028 ∠-15.9°	1.0355 ∠-15.4°	1.0326 ∠-9.8°
28	1.01 ∠-11.7°	1.0175 ∠-11.2°	1.0134 ∠-5.5°
29	1.009 ∠-17.1°	1.0159 ∠-16.6°	1.013 ∠-11°
30	0.995 ∠-18°	1.0046 ∠-17.5°	1.0016 ∠-11.9°
V_{CP}	-	1.0227 ∠-7.4°	1.0227 ∠-3.2°
V_S	-	0.9854 ∠-9.2°	1.0158 ∠-3.4°
V_R	-	1.0768 ∠-7.0°	1.0191 ∠-3.3°

Table 4: Results of power flow control of IEEE 30 bus power system on each branch

TL x-y	Base case		Case (1)		Case (2)	
	P (MW)	Q (MVAr)	P (MW)	Q (MVAr)	P (MW)	Q (MVAr)
1-2	173	-21	181.3	-22.96	85.81	1.57
1-3	88	4.3	78.79	1.36	45.15	8.55
2-4	44	3.5	30.51	2.33	23.6	6.03
2-5	82.1	1.8	73.42	2.55	53	4.95
2-6	59.9	-0.1	-	-	26.25	6.12
$2\text{-}6_{S\text{-}R}$	-	-	90	40	-	-
3-4	82.5	-3.9	73.88	-4.53	41.88	8.62
4-6	68.5	-17	48.56	-18.67	12.61	0.736
4-12	48.5	14.1	47.05	16.18	44.71	15.44
5-7	-15	11.2	-23.13	8.95	-42.44	15.34
6-7	38.4	-2.5	46.77	0.552	-	-
$6\text{-}7_{S\text{-}R}$	-	-	-	-	60	-10
6-8	29.8	-5.6	29.66	20.86	29.97	4.15
6-9	17.2	-1.8	17.67	-0.572	18.54	-1.36
6-10	20.4	0.2	20.99	1.31	22	0.59
6-28	20	-10.4	20.52	-6.32	20.79	-9.08
8-28	-0.3	-2.3	-0.295	-6.44	-0.142	-3.86
9-10	17.2	9.1	17.67	8.06	18.54	8.28
9-11	0	-12.5	0	-10.2	0	-11.39
10-17	2.9	5.6	3.58	5.81	4.69	5.25

TL x-y	Base case		Case (1)		Case (2)	
	P (MW)	Q (MVAr)	P (MW)	Q (MVAr)	P (MW)	Q (MVAr)
10-20	7.7	4.4	8.04	4.51	8.61	4.18
10-21	14.5	10.6	14.47	10.58	14.6	10.59
10-22	6.8	5	6.76	4.99	6.85	4.99
12-13	0	-9.2	0	-6.38	0	-7.91
12-14	8.2	2.1	8.02	2.03	7.8	2.22
12-15	19.5	5.9	18.81	5.71	17.82	6.28
12-16	9.7	2.3	9.02	2.03	7.89	2.54
14-15	1.9	0.3	1.74	0.279	1.53	0.472
15-18	7.4	0.9	7	0.793	6.44	1.12
15-23	5.6	2.4	5.13	2.23	4.5	2.71
16-17	6.1	0.3	5.45	0.075	4.33	0.621
18-19	4.1	-0.1	3.75	-0.207	3.19	0.139
19-20	-5.4	-3.6	-5.76	-3.62	-6.31	-3.27
21-22	-3.1	-0.8	-3.13	-0.834	-3	-0.83
22-24	3.6	4.1	3.59	4.06	3.8	4.06
23-24	2.3	0.7	1.9	0.588	1.28	1.06
24-25	-2.8	2.6	-3.25	2.46	-3.66	2.91
25-26	3.5	2.4	3.54	2.37	3.54	2.37
25-27	-6.4	0.2	-6.82	0.042	-7.25	0.475
27-28	-20	-3.2	20.14	4.9	-20.58	-2.95
27-29	6.2	1.7	6.19	1.66	6.19	1.66
27-30	7.1	1.7	7.09	1.66	7.09	1.66
29-30	3.7	0.6	3.7	0.6	3.7	0.6

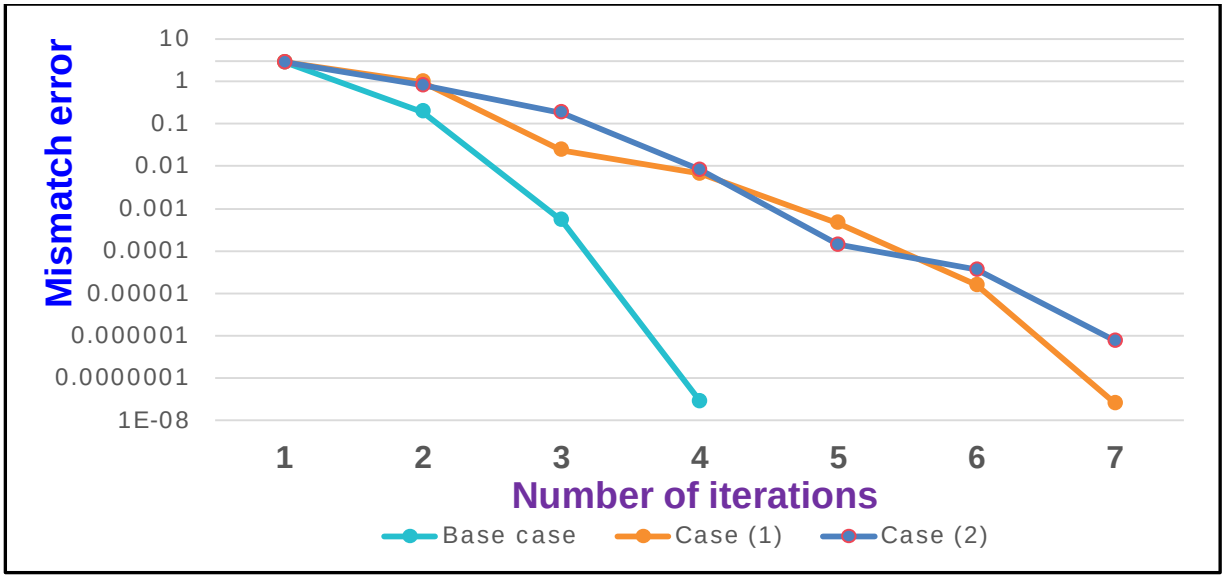

Figure 8: Iterations of load flow analysis for IEEE 30 bus cases.

5 Conclusion

This paper introduced a NEPLAN software-established C-UPFC model. This model implemented using the existed components in that software. The primary goal is to integrate a model of C-UPFC device for power flow calculations for systems involving such a device in NEPLAN software. Such a model is assessed in two power systems: IEEE 14 bus and IEEE 30 bus systems. For both systems, the model was installed in two different cases, including changing its position and control setting. It was tested so that it can provide active and reactive power flow control over the desired TL, besides controlling the center node voltage. For IEEE 14 bus, the load flow calculations were settled after 10 iterations for case 1, while it was settled after 11 iterations for case 2. On the other side, the load flow calculations were settled after 7 iterations in IEEE 30 bus for both cases. Such results show that the model was successfully simulated and it assures its versatility,

robustness, and effectiveness for load flow calculations so that it can be drastically utilized for power system analyses incorporating such a device in NEPLAN software.

6 Availability of Data and Material

Information can be made available by contacting the corresponding author.

7 References

[1] Narain G. Hingorani and L. Gyugyi. (2000). *Understanding FACTS: Concepts and Technology of Flexible AC Transmission Systems*. 1st ed., Vol. 1. New York: IEEE Press.

[2] Sode-Yome, A., N. Mithulananthan, and Kwang Y. Lee. (2007). A comprehensive comparison of FACTS devices for enhancing static voltage stability. IEEE Power Engineering Society General Meeting. 1-8. IEEE.

[3] Asawa S., and S. Al-Attiyah. (2016). Impact of FACTS device in electrical power system *International Conference on Electrical, Electronics, and Optimization Techniques (ICEEOT)*. 2488-2495. IEEE.

[4] Albatsh, F. M. et al. (2015). Enhancing power transfer capability through flexible AC transmission system devices: a review. *Frontiers of Information Technology & Electronic Engineering*, 16(8), 658-678.

[5] Komoni, V. et al. (2010). Increase power transfer capability and controlling line power flow in power system installed the FACTS. *7th Mediterranean Conference and Exhibition on Power Generation, Transmission, Distribution and Energy Conversion*. 193-199.

[6] Kamel, S. and F. Jurado. (2015). Modeling of STATCOM in load flow formulation. Static Compensators (STATCOMs) in Power Systems. 405-435. Springer, Singapore.

[7] Zhang, Y. et al. (2006). Power injection model of STATCOM with control and operating limit for power flow and voltage stability analysis. *Electric Power Systems Research*. 76(12), 1003-1010.

[8] Ebeed, M., S. Kamel and F. Jurado. (2017). Constraints violation handling of SSSC with multi-control modes in Newton–Raphson load flow algorithm. *IEEJ Transactions on Electrical and Electronic Engineering*. 12(6), 861-866.

[9] Awad, A. et al. (2019). A Simple Modeling of Static Series Synchronous Compensator in NEPLAN for Power System Control. *IECON 2019-45th Annual Conference of the IEEE Industrial Electronics Society*. 7033-7037. IEEE.

[10] Zhang, Y., Y. Zhang and C. Chen. (2006). A novel power injection model of IPFC for power flow analysis inclusive of practical constraints. *IEEE Transactions on Power Systems*. 21(4), 1550-1556.

[11] Ghane, H. and S. K. Y. Nikravesh. (2009). A nonlinear C-UPFC control design for power transmission line applications. *Proceedings of the International MultiConference of Engineers and Computer Scientists*, 2.

[12] Rashad, A. et al. (2018). Performance improvement of various types of induction-based wind farms using center-node unified power flow controller. *International Journal of Control, Automation and Systems*. 16(6), 2644-2655.

[13] Ajami, A. et al. Gharehpetian. (2006). Modeling and control of C-UPFC for power system transient studies. *Simulation Modelling Practice and Theory*. 14(5), 564-576.

[14] Kamel, S. et al. (2018). A comprehensive model of C-UPFC with innovative constraint enforcement

techniques in load flow analysis. *International Journal of Electrical Power & Energy Systems.* 101, 289-300.

[15] Kamel, S., F. Jurado and R. Mihalic. (2015). Advanced modeling of center-node unified power flow controller in NR load flow algorithm. *Electr Power Syst Res.* 121, 176-182.

[16] Power systems test case archive. University of Washington, Seattle (Online). http://labs.ece.uw.edu/pstca/pf14/ieee14cdf.txt Accessed April 2020.

[17] Power systems test case archive. University of Washington, Seattle (Online). http://labs.ece.uw.edu/pstca/pf30/ieee30cdf.txt Accessed April 2020.

A. Awad received his B.Sc degree in Electrical Engineering from Higher Technological Institute (HTI), 10th of Ramadan city, and received his M.Sc degree from Aswan University. He is currently pursuing a jointly supervised Ph.D. degree in electrical engineering between the University of Jaen, Spain and Aswan University, Egypt. His research interest includes Optimization Techniques, Renewable Energy, and Smart Grids.

Dr.Salah Kamel is an Associate Professor in the Electrical Engineering Department, Aswan University. He received a joint Ph.D. degree from the University of Jaen, Spain (Main) and Aalborg University, Denmark (Host). His research includes power System Analysis and Optimization, Smart Grid, and Renewable Energy Systems.

Dr.Ali S. Alghamdi is an Assistant Professor and Acting Chair, the Department of Electrical Engineering, the College of Engineering, Majmaah University, Saudi Arabia. He received his dual B.S. degree (with high honors) in Computer and Electrical Engineering from Lawrence Technological University, Southfield, Michigan, USA, respectively, and an MSc in Electrical and Computer Engineering from Lawrence Technological University, Southfield, Michigan, USA. He received a Ph.D. in Electrical and Computer Engineering from Oakland University, Rochester, Michigan, USA. His research interests include Statistical Digital Signal Processing, Communication Systems, Adaptive Filter, Modern Control in Power System, Optoelectronics Nano-materials in Renewable Energy, and Wireless Sensor Network Innovation.

Professor Dr.Francisco Jurado is a Full Professor at the Department of Electrical Engineering of the University of Jaén, Spain. He obtained the MSc and Ph.D. degrees from the UNED, Madrid, Spain. His research activities have focused on Power Systems and Renewable Energy.

Professor Dr.Mohamed Zohdy works at Oakland University, Michigan, USA. He received his B.Sc. degree in Electrical Engineering, Cairo University, Egypt. He received his M.Sc. and Ph.D. degrees in Electrical Engineering, University of Waterloo, Canada. His interests are Control and Soft Computing.